Biochemistry and Biophysics Reports 12 (2017) 158–165

Contents lists available at ScienceDirect

Biochemistry and Biophysics Reports

journal homepage: www.elsevier.com/locate/bbrep

Temperature and osmotic stress dependence of the thermodynamics for binding linker histone $H1^0$, Its carboxyl domain ($H1^0$-C) or globular domain ($H1^0$-G) to B-DNA

V.R. Machha[b], C.G. Mikek[a], S. Wellman[c], E.A. Lewis[a,*]

[a] Department of Chemistry, Mississippi State University, Mississippi, MS 39762, USA
[b] Division of Hematology, Departments of Internal Medicine and Biochemistry and Molecular Biology, Mayo Clinic, Rochester, MN 55905, USA
[c] Department of Pharmacology and Toxicology, University of Mississippi Medical Center, 2500 N. State Street, Jackson, MS 39216, USA

ARTICLE INFO

Keywords:
Histone
$H1^0$
$H1^0$-C
$H1^0$-G
CT-DNA
Chromatin
Nucleosome
ITC
CD

ABSTRACT

Linker histones (H1) are the basic proteins in higher eukaryotes that are responsible for the final condensation of chromatin. In contrast to the nucleosome core histone proteins, the role of H1 in compacting DNA is not clearly understood. In this study ITC was used to measure the binding constant, enthalpy change, and binding site size for the interactions of $H1^0$, or its C-terminal ($H1^0$-C) and globular ($H1^0$-G) domains to highly polymerized calf-thymus DNA at temperatures from 288 K to 308 K. Heat capacity changes, ΔC_p, for these same $H1^0$ binding interactions were estimated from the temperature dependence of the enthalpy changes. The enthalpy changes for binding $H1^0$, $H1^0$-C, or $H1^0$-G to CT-DNA are all endothermic at 298 K, becoming more exothermic as the temperature is increased. The ΔH for binding $H1^0$-G to CT-DNA is exothermic at temperatures above approximately 300 K. Osmotic stress experiments indicate that the binding of $H1^0$ is accompanied by the release of approximately 35 water molecules.

We estimate from our naked DNA titration results that the binding of the $H1^0$ to the nucleosome places the $H1^0$ protein in close contact with approximately 41 DNA bp. The breakdown is that the $H1^0$ carboxyl terminus interacts with 28 bp of linker DNA on one side of the nucleosome, the $H1^0$ globular domain binds directly to 7 bp of core DNA, and shields another 6 linker DNA bases, 3 bp on either side of the nucleosome where the linker DNA exits the nucleosome core.

1. Introduction

Linker histone H1 mediates DNA packaging alongside the core histone octamer by binding to both the linker DNA and nucleosomal DNA to further condense the chromatin [1]. The linker histone's basic structure is composed of three domains, a short disordered N-terminal domain approximately 35 amino acid residues in length, a central globular winged helix domain approximately 65 residues in length, and a longer disordered C-terminal domain approximately 100 amino acid residues in length [2,3]. Although several studies have focused on H1 interactions with both nucleosomal DNA and naked DNA, this study represents the first attempt to thermodynamically characterize the $H1^0$, $H1^0$-C, and $H1^0$-G interactions with DNA over a range in temperature. In a previous study we used isothermal titration calorimetry (ITC) to determine the thermodynamics for binding of $H1^0$, $H1^0$-C, and $H1^0$-G to highly polymerized calf-thymus DNA at 298 K in solutions containing a nominal salt concentration of approximately 0.1 M [4]. In our previous ITC studies [4], we found that the intact protein ($H1^0$) and its C-terminal domain ($H1^0$-C) bind to CT-DNA with approximately the same high affinity ($K_a \approx 1 \times 10^7$). We also observed large unfavorable enthalpy changes for the formation of these H1•DNA complexes ($\Delta H \approx +22$ kcal/(mol $H1^0$ or $H1^0$-C)) [4]. There was no significant heat change observed for the addition of $H1^0$-G to CT-DNA at 298 K indicating that the $H1^0$-G•DNA complex was either not formed or formed with a very small change in enthalpy at this temperature ($\Delta H \approx 0$ kcal/(mol $H1^0$-G)). On the other hand, CD measurements indicated significant binding between $H1^0$-G and CT-DNA. The free energy change for formation of the $H1^0$•DNA and $H1^0$-C•DNA complexes at 298 K is driven by a very favorable entropy change ($-T\Delta S \approx -30$ kcal/mol), and the binding site sizes for $H1^0$ and $H1^0$-C were determined to be 36 bp and 28 bp, respectively [4]. The binding affinity and binding site size determined here for formation of the $H1^0$•CT-DNA complex are in reasonable agreement with the results of Mamoon et al. and Watanabe [5,6]. Using the polyelectrolyte theory of Record *et al.* the electrostatic

Abbreviations: ITC, Isothermal Titration Calorimetry; CD, Circular Dichroism; CT-DNA, Calf Thymus DNA

* Corresponding author.

http://dx.doi.org/10.1016/j.bbrep.2017.09.009
Received 4 August 2017; Received in revised form 21 September 2017; Accepted 25 September 2017
Available online 13 October 2017

contribution to the free energy change for binding $H1^0$ or $H1^0$-C to CT-DNA, ΔG_{elec}, was estimated to range from 6% to 17% of the total ΔG. In addition, the release of bound counterions (e.g. K^+) upon formation of the $H1^0$ and $H1^0$-C•CT-DNA complexes was estimated to be only one potassium ion [4]. We speculated that the large favorable entropy term for the formation of the $H1^0$•DNA and $H1^0$-C•DNA complexes was due largely to the expulsion of bound water molecules from the protein•DNA interaction interface.

In the present study, we performed ITC titration experiments over the temperature range of 288–313 K. In contrast to ITC experiments previously performed at 298 K where ΔH was found to be approximately zero for formation of the $H1^0$-G•CT-DNA complex, we noted that ΔH for formation of the $H1^0$-G•CT-DNA complex at higher temperatures was exothermic with $\Delta H \approx -8$ kcal/(mol $H1^0$-G) at 313 K. Analysis of $H1^0$-G•CT-DNA ITC data (at 313 K), using our fractional sites binding model, suggests that the binding mechanism for the interaction of the $H1^0$-G with CT-DNA may involve the formation of two different complexes.

The ITC experiments performed at different temperatures allowed us to determine ΔCp values for the formation of the $H1^0$ and $H1^0$-C•CT-DNA complexes. The ΔCp values determined here were found to be large and negative ($\Delta Cp \approx -430$ cal mol^{-1} K^{-1}). This result is consistent with the loss of structure in the protein or DNA and/or the loss of bound water molecules as these complexes are formed. In this study, we also performed ITC experiments with TEG (triethylene glycol) added as a co-solute or osmolyte. These experiments performed at osmolalities of 0.2–1.4 osmolal allowed us to probe the role of water and water release in the formation of the $H1^0$•CT-DNA complex. The result of the osmotic stress experiments is that the overall change in hydration, (ΔN_w), for formation of the $H1^0$•CT-DNA complex is –35 ± 8 water molecules. In effect, approximately 35 water molecules are released upon complex formation. Obviously the estimated values for ΔCp and ΔN_w are in good agreement.

2. Materials and methods

The $H1^0$ intact protein and its C-terminal and Globular domains were expressed using a bacterial strain of *E.coli* (*Rosetta2 (De3) pLysS*) transformed with a pET-11d (Novagen) expression vector as described previously. [7] The constructions of the expression strains, induction, extraction, and purification have been described. [4,8] The pure protein fractions were lyophilized using a Savant SPD 111 V Speed-Vac system for 4 h at 308 K and dissolved in 2 mL of sample buffer. Typically the sample buffer was BPES (30 mM [K_2HPO_4/KH_2PO_4] pH = 7.0, 1 mM EDTA, 100 mM KCl). For the osmotic stress dependent studies, osmolyte, i.e. TEG, was added to yield solutions of 0.2 *m*, 0.4 *m*, 0.6 *m*, 0.8 *m*, 1.0 *m*, 1.2 *m*, and 1.4 *m*. Calf thymus DNA type I was purchased from Sigma (St. Louis, USA) and dissolved in 1 mL of the sample buffer. Both protein and DNA stock solutions were exhaustively dialyzed against the sample buffer (24 h) at 277 K. DNA concentrations in base pairs (bp) were determined using measured absorbance at 260 nm and a molar extinction coefficient of $\varepsilon_{260} = 1.31 \times 10^4$ bp $M^{-1}cm^{-1}$.[9] The concentrations of $H1^0$, $H1^0$-C and $H1^0$-G were calculated using extinction coefficients 27.8, 31.1, and 28.6 mL mg^{-1} cm^{-1}, respectively at 205 nm. [7]

The approximate molecular weights for the H1 and H1 domain constructs were estimated from their sequences using the ExPASy ProtParam tool (http://web.expasy.org/protparam): Mw ($H1^0$) ≈ 20.8 kDa, Mw ($H1^0$-C) ≈ 9.55 kDa, Mw ($H1^0$-G) ≈ 9.28 kDa. The approximate average molecular weight of the CT-DNA was 8.42×10^3 kDa (Sigma, St. Louis, USA).

Isothermal titration calorimetry (ITC) experiments were performed using a Microcal VP-ITC (Northampton, MA, USA). All titrations were performed by overfilling the ITC cell with approximately 1.5 mL of a dilute CT-DNA solution (nominally 480 μM in bp). Approximately 300 μL of a dilute solution of $H1^0$ (nominally 150 μM) was titrated into the calorimeter cell. The injection volume in these titrations was nominally 10 μL and a typical titration involved 30 injections of titrant at 600 s intervals. Titrations were performed at five different temperatures (i.e., 288, 293, 298, 303, and 308 K). All of the ITC experiments were performed in triplicate. The integrated heat/injection data were fit to appropriate thermodynamic models using CHASM data analysis software developed in our laboratory. [10] The non-linear regression fitting process yields best fit parameters for *K* (or ΔG), ΔH, ΔS, and n.

The osmotic stress experiments were done in the presence of added osmolyte solution. Osmolyte (TEG) solutions were prepared by weight to achieve nominal osmolality ranging from 0.2 to 1.4 m. The final osmolyte concentrations of the solutions were measured on a Wescor 5560 (Logan, UT).

HPLC/ESI-MS experiments were performed using a Dionex (Sunnyvale, CA, USA) uHPLC coupled to a Bruker (Bellirica, MA, USA) MicrOTOFQ mass spectrometer. Negative ion mode was utilized for DNA samples while positive ion mode was utilized for both protein analysis and protein/DNA sample solutions. These samples prepared in KBPES buffer were injected into the uHPLC system by the autosampler and excess salts were flushed out of the uHPLC system in the first 10 min. Gradient flow from 100% acetic acid to 95% acetonitrile was used. The MS capillary voltage was set to +3500 V, dry N2 gas flow was adjusted to 9 L/min at 453 K. Data processing was performed by using Bruker Daltonics Data Analysis program.

Molecular modeling and MD simulations were performed using Accelrys Discovery Studio v.3.1 (San Diego, CA, USA). Since there is no known crystallographic or solution structure for H1-Globular domain, H5-G was used instead to model the H1-G due to very high sequence identity (78%). The structure for the H1-Globular domain was adapted and modified from the Protein Data Bank (PDB accession code 1HST) [11]. The H1-Globular domain was typed with the CHARMm27 forcefield using the Momany-Rone partial charge method. The entire system was solvated using an Explicit Periodic Boundary condition with an orthorhombic shell extending 10 Å away from the boundary. Counterions were added to a concentration of 0.15 M. The system was subjected to a minimization routine using the Smart Minimizer algorithm and involving as many as 8000 steps using a RMS gradient of less than 0.1 and a spherical cutoff electrostatics model.

DNA-protein interactions were modeled with the proposed binding sites based on a homology model as described by Ramakrishnan *et al.* [11] A nucleosomal B-DNA fragment was extracted from the X-ray structure of nucleosome core particle (PDB accession code 1AOI) and was used as a substrate for linker histone protein binding. Based on the homology binding model described by Ramakrishnan *et al.*, there are two possible H1-G binding sites. Following Ramakrishnan's model, residues from the H1-globular domain were manually brought into contacts with the major groove of DNA. The Intermolecular Monitor feature was employed to assist with visualizing the intermolecular contacts between the protein residues and the bases in the major groove. Specifically, for the primary binding site, residues Lys69, Lys85, and Arg73 are bought in close proximity with the DNA grooves, while in the hypothetical secondary binding site, residues Lys40, Arg42, Lys52, and Arg94 are brought to close proximity with the DNA grooves. The protein-DNA complex was again subjected to minimization routines as described above.

3. Results

The heat capacity changes (ΔCp) associated with the binding interactions of either $H1^0$ or $H1^0$-C to CT-DNA can be determined directly from the temperature dependence of binding enthalpy using the equation $\Delta Cp = \delta(\Delta H)/\delta T$ [12]. We performed a temperature dependent study utilizing ITC experiments in which $H1^0$ or $H1^0$-C were titrated into CT-DNA at temperatures ranging from 288 K to 308 K. The ITC thermograms at various temperatures were fit using nonlinear

Table 1
Thermodynamic parameters for binding $H1^0$ and $H1^0$-C to CT-DNA.

	Temp (K)	$K_a \times 10^{-7}$ (M^{-1})	ΔG (kcal/mol)	ΔH (kcal/mol)	–TΔS (kcal/mol)
$H1^0$	288	1.6 ± 0.2	–9.5	22.9 ± 0.2	–32.4
	293	1.6 ± 0.1	–9.5	21.9 ± 0.3	–31.5
	298	0.7 ± 0.1	–9.4	21.2 ± 0.1	–31.0
	303	0.6 ± 0.1	–9.1	16.6 ± 0.3	–26.4
	308	0.5 ± 0.1	–9.2	14.6 ± 0.5	–23.5
$H1^0$-C	288	1.7 ± 0.1	–9.6	24.1 ± 0.4	–33.6
	293	1.7 ± 0.2	–9.6	21.9 ± 0.2	–31.6
	298	0.6 ± 0.1	–9.1	20.6 ± 0.2	–29.8
	303	1.6 ± 0.2	–9.5	16.8 ± 0.3	–26.3
	308	1.6 ± 0.1	−9.5	15.9 ± 0.3	−25.1

ITC derived thermodynamic parameters for $H1^0$ and $H1^0$-C binding to CT-DNA at 288, 293, 298, 303, and 308 K in 100 mM KBPES buffer at pH 7.0. Errors listed are the standard deviations for the best fit parameters *K* and ΔH determined in triplicate ITC experiments and fit to a one site binding model.

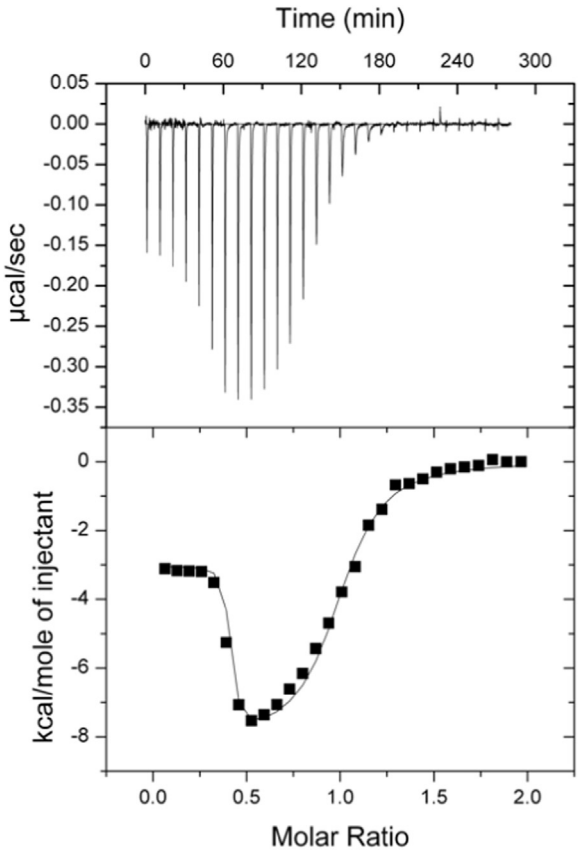

Fig. 1. A typical ITC titration for the addition of $H1^0$-G to highly polymerized CT-DNA at 313 K. The upper half of panel shows the baseline-corrected raw ITC signal for 30 injections of a dilute $H1^0$-G protein solution (10 µL of 169 µM $H1^0$-G) into the ITC cell filled with a dilute solution of CT-DNA (122 µM bp or 17.4 µM in $H1^0$-G binding sites). The lower half of panel shows the apparent ΔH for each injection (-■-) along with the best-fit non-linear regression line (—) for a fractional sites binding model. Derived thermodynamic parameters resulted from these fits are listed in Table 2.

regression techniques to an independent site model (one site model) and the average best-fit parameters are listed in Table 1.

Fig. 1 shows both the raw ITC signal (upper panel) and the apparent heat data for the titration of the $H1^0$-G into CT-DNA at 313 K. The integrated heat data were fit using a "fractional-sites" binding model where the total number of protein binding sites was set to one (i.e. saturation stoichiometry of 1 mol of protein per 1 mol of binding site). The size of a protein binding site was determined to be 7 DNA base pairs from the ITC endpoint and the concentration of DNA in bp. The thermogram is consistent with the formation of two different $H1^0$-G•DNA complexes. The first complex formation is accompanied by a smaller change in enthalpy than the second complex at the same temperature. The nonlinear regression fit of the heat data to a fractional sites model (shown as the solid line in Fig. 1) revealed the stoichiometries for the formation of the high affinity and lower affinity complexes to be 0.34 and 0.63 respectively. Table 2 lists the best fit thermodynamic parameters for the formation of the $H1^0$-G•CT-DNA complex at 298, 303, 308, and 313 K. The interaction between the $H1^0$-G and CT-DNA is calorimetrically silent at 298 K (ΔH ≈ 0 kcal/mol); however, values for ΔG and -TΔS can be extrapolated from 313, 308, and 303 K back to 298 K. In Table 2, the ΔG_i, ΔH_i, and $-T\Delta S_i$ values extrapolated to 298 K are indicated with asterisks.

Values for the ITC determined enthalpy changes are listed in Tables 1 and 2 and are shown as a function of temperature in Fig. 2. The ΔH values for binding both $H1^0$ and $H1^0$-C to CT-DNA exhibit a similar linear decrease in the endothermic enthalpy change with increasing temperature. The slope of the least square line in Fig. 2 for binding either $H1^0$ or $H1^0$-C to CT-DNA corresponds to an estimated value for ΔC_p of -430 cal mol^{-1} K^{-1}. Since formation of the second $H1^0$-G•CT-DNA complex represents the predominant (66%) complex species in the $H1^0$-G titration experiments, ΔH_2 for formation of the second $H1^0$-G•CT-DNA complex was chosen to be plotted against the temperature. The slope of the least square line for binding $H1^0$-G to CT-DNA corresponds to an estimated value for ΔC_p of -590 cal mol^{-1} K^{-1}.

In Fig. 3 we have plotted the values of (ΔH_t - $\Delta H_{average}$), (ΔG_t - $\Delta G_{average}$), and (-$T\Delta S_t$ – (-$T\Delta S_{average}$)) for the binding of $H1^0$ and $H1^0$-C to CT-DNA as a function of temperature. The enthalpy change for formation of the $H1^0$•CT-DNA and $H1^0$-C•CT-DNA complexes are increasingly exothermic as the temperature is increased, while the entropy change is increasingly less favorable at higher temperatures. The changes in ΔH (δΔH ≈ 8 kcal/mol) and –TΔS (δ-TΔS ≈ 9 kcal/mol) over the temperature range 288–308 K compensate one another and the change in free energy, ΔG, with temperature is buffered (δΔG ≈ 0.5 kcal/mol).

In Fig. 4 we have plotted the values of ($\Delta H_{i,t}$ - $\Delta H_{i,average}$), ($\Delta G_{i,t}$ - $\Delta G_{i,average}$), and (-$T\Delta S_{i,t}$ – (-$T\Delta S_{i,average}$)) for the binding of $H1^0$-G to CT-DNA as a function of temperature. The enthalpy change for both binding processes (1 and 2) for formation of the $H1^0$-G•CT-DNA complex are increasingly exothermic (favorable) as the temperature is increased, while the entropy change is increasingly less favorable at higher temperatures. Once again, the changes in ΔH (δΔH ≈ 9 kcal/mol) and –TΔS (δ-TΔS ≈ 10 kcal/mol) over the temperature range 298–313 K compensate one another and the change in free energy, ΔG, with temperature is buffered (δΔG ≈ 1 kcal/mol).

In our earlier study we determined the thermodynamic parameters and the binding site sizes for $H1^0$ and $H1^0$-C binding to CT-DNA at 298 K [4]. We also attempted to measure the interaction between $H1^0$-G and CT-DNA, but the interaction is calorimetrically silent at 298 K. In this study, we estimated the thermodynamic signatures for the binding of $H1^0$-G to CT-DNA at 298 K from the extrapolation of the fitting parameters (ΔG, ΔH, and -TΔS) at higher temperatures back to 298 K. In our previous work, only a single complex formation was observed for the binding of either $H1^0$ or $H1^0$-C to CT-DNA [4]. However, the ITC thermogram shown in Fig. 1 for the binding of $H1^0$-G to CT-DNA at higher temperatures (303, 308, and 313 K) clearly indicates formation of two complexes with characteristic thermodynamic signatures. We speculate that in the intact $H1^0$ protein, the dynamic nature of the globular domain is restricted by both the N- and C-domains therefore limiting its interaction with CT-DNA.

To further verify the binding site size for complexation of $H1^0$-G to duplex DNA, we performed ITC and ESI-MS experiments with short oligomers (7 bp and 14 bp). ITC results obtained for 7 bp and 14 bp oligomers (data not shown) are very similar to results obtained for the CT-DNA and produced the expected stoichiometry indicating 7 bp of ds-DNA occupied by 1 mol of $H1^0$-G protein. Typical HPLC chromatograph

Table 2
Thermodynamic parameters for $H1^0$-G binding to CT-DNA.

Temp (K)	K_1 (M^{-1}) $\times 10^{-9}$	ΔG_1 (kcal/mol)	ΔH_1 (kcal/mol)	$-T\Delta S_1$ (kcal/mol)	K_2 (M^{-1}) $\times 10^{-6}$	ΔG_2 (kcal/mol)	ΔH_2 (kcal/mol)	$-T\Delta S_2$ (kcal/mol)
313	2.9 ± 1.6	−12.9	−2.9 ± 0.3	−9.9	2.4 ± 1.6	−8.7	−8.1 ± 0.5	−0.6
308	1.4 ± 1.0	−12.5	−1.1 ± 0.1	−11.3	3.3 ± 2.5	−8.9	−4.6 ± 0.2	−4.3
303	0.9 ± 0.6	−12.2	−0.3 ± 0.1	−12.6	13 ± 10	−9.7	−2.2 ± 0.3	−7.5
298	–	−11.8*	1.2*	−13.0*	–	−10.1*	0.9*	−11.0*

ITC derived thermodynamic parameters for $H1^0$-G binding to CT-DNA at 303, 308, and 313 K in 100 mM [K^+] BPES pH 7.0. Errors listed are the standard deviations for the best fit parameters *K* and ΔH determined in triplicate experiments.

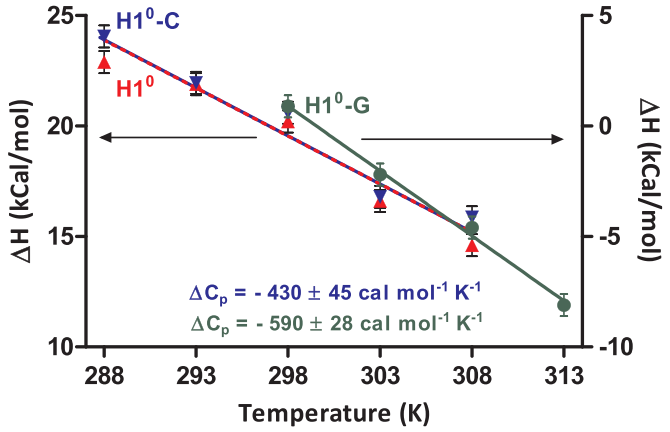

Fig. 2. A plot of the ITC derived ΔH values for the formation of the $H1^0$, $H1^0$-G, and $H1^0$-C•CT-DNA complexes vs. temperature. The slopes of the two overlapping lines yield estimates for the ΔCp values that accompany the formation of the $H1^0$ and $H1^0$-C CT-DNA complexes. $H1^0$-G•CT-DNA data for the lower affinity predominant species is also shown (see text).

ESI mass spectra for free $H1^0$-G and $H1^0$-G•7 bp or $H1^0$-G•14 bp dsDNA and are shown in Fig. 5.

The effect of increased concentrations of TEG on the binding was measured by ITC at 298 K. Thermodynamic parameters obtained from fitting ITC titrations performed at different concentrations of osmolyte ranging from 0.2 to 1.4 *m* were plotted in Fig. 6.

This plot demonstrates that the binding free energies are only weakly dependent on the osmolality of the solution. The binding of $H1^0$ to CT-DNA at higher osmolyte (TEG) concentrations was found to be enthalpically more favorable. However the favorable change in enthalpy is offset by an unfavorable change in entropy. In Fig. 7 we have plotted the natural logarithm of the K_a values as a function of osmolyte concentrations to determine the net hydration change. Osmolyte dependence of the equilibrium constant coupled with hydration changes has been analyzed by the following equation [13]

$$\delta(\ln K)/\delta(Osm) = -\Delta N_w/55.6 \quad (1)$$

Where K_a is the equilibrium constant, Osm is the osmolality (moles of cosolute/kg of buffer) of the buffer, and ΔN_w is the change in the number of water molecules for the association of $H1^0$ with CT-DNA. A linear-least-square fit of the data points in Fig. 7 using Eq. (1) gives ΔN_w value as -35 ± 8. In effect, a net value of 35 water molecules are released upon formation of $H1^0$•CT-DNA complex.

Results of the docking study are presented in Fig. 8 for the formation of two different $H1^0$-G•DNA complexes. Again, the contact residues between the protein and DNA are modeled after Ramakrishnan et al. [11] Several observations can be made from the modeling study. In the first proposed binding model, duplex DNA can remain in linear conformation without losing any contacts with the three amino acid residues K69, R73, and K85. However, a linear B-DNA cannot effectively faciliate contacts with all proposed residues in the second binding model. The second binding model utilizing four amino acid residues (K40, R42, K52, and R94) requries the B-DNA to be bent slightly in order to make contacts with the DNA backbones. Furthermore, in the first binding model, the majority of three contact residues are located on helix III; while in the second binding model, the four contact residues are located on helix I and II. Finally, in the first model, recognition helix III binding to the major groove of the ds-DNA appears to be bidirectional, in effect the $H1^0$-G can bind the duplex DNA in either the 5′ to 3′ direction or 3′ to 5′ direction. In constrast, contact residues located in helices I and II appear to bind unidirectianlly with ds-DNA in the second binding model. Unidirectionality and bidirectionalality are being discussed in the context that all proposed contact residues (either K69, R73, and K85 or K40, R42, K52, and R94) must form favorable interactions with the DNA.

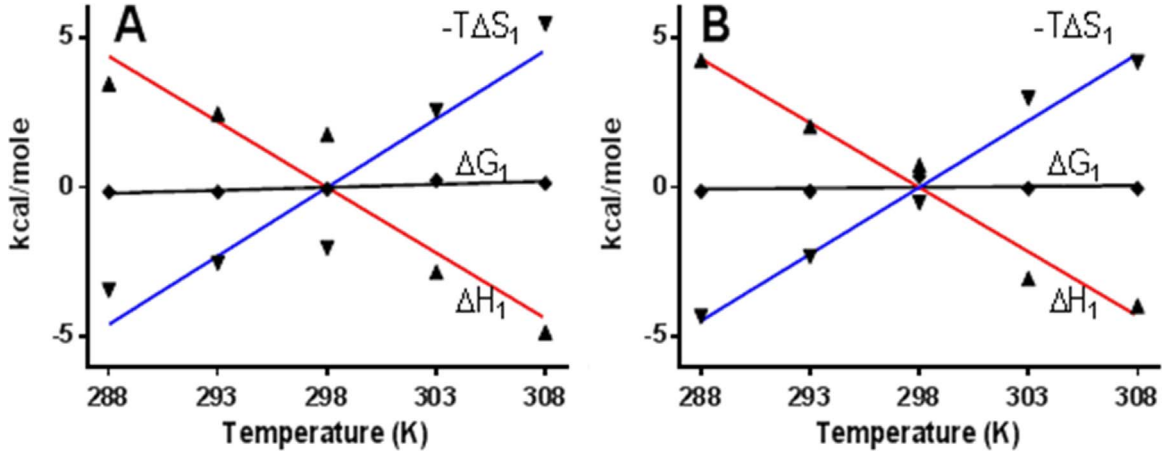

Fig. 3. A plot of the thermodynamic parameters, ΔG, ΔH, and –TΔS for the binding of (A) $H1^0$ to CT-DNA and (B) $H1^0$-C to CT-DNA as a function of temperature (Values plotted as (ΔH_t - $\Delta H_{average}$), (ΔG_t - $\Delta G_{average}$), and ($-T\Delta S_t$ – ($-T\Delta S_{average}$)).

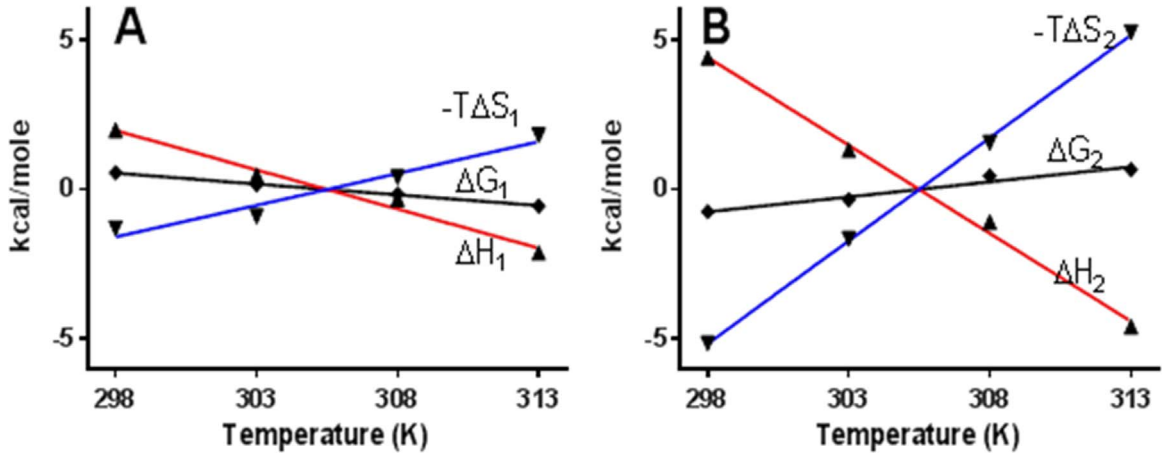

Fig. 4. A plot of the thermodynamic parameters, ΔG, ΔH, and –TΔS for the formation of high affinity complex (A) and lower affinity complex (B) for the binding of H1^0-G to CT-DNA as a function of temperature (Values plotted as (ΔH_t - $\Delta H_{average}$), (ΔG_t - $\Delta G_{average}$), and (-TΔS_t – (-T$\Delta S_{average}$)).

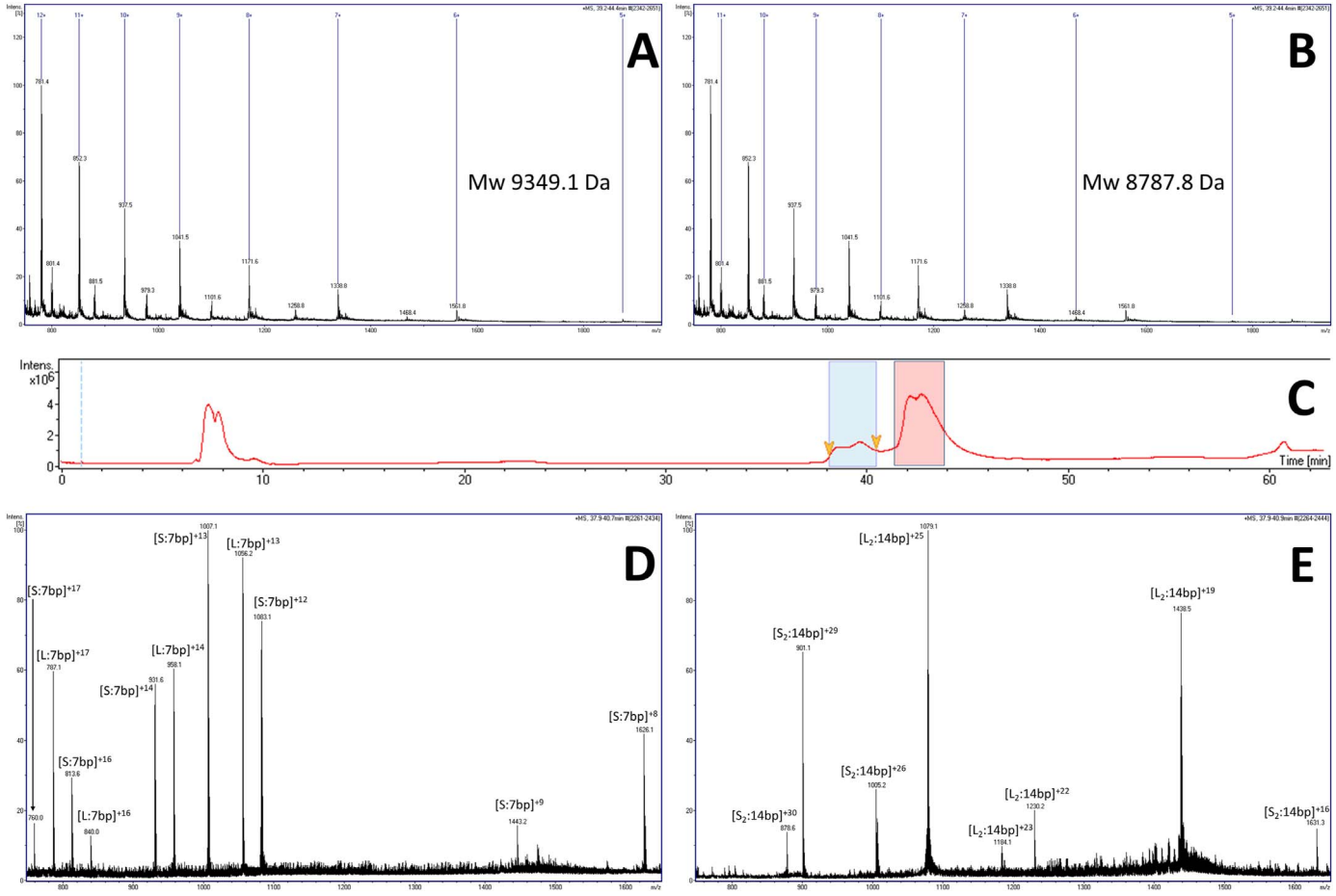

Fig. 5. ESI mass spectra analysis for the free H1^0-G protein utilizing the charge state ruler tool from Bruker Daltonics Data Analysis program. Panel A shows the mass analysis for a full length (L) 86 amino acids H1^0-G protein. Panel B shows the mass analysis for a shorter (S) 81 amino acids H1^0-G protein with RSVAF residues truncated from the C-terminus. Panel C shows a typical HPLC trace for solutions containing either the H1^0-G•7 bp complex or H1^0-G•14 bp complex. The turquoise box indicates the elution region for either the H1^0-G•7 bp complex or H1^0-G•14 bp complex. The red box indicates the elution region of excess (unbound) H1^0-G protein. Panel D shows the ESI mass spectra analysis for H1^0-G•7 bp complex. Panel E shows the ESI mass spectra analysis or H1^0-G•14 bp complex.

4. Discussion

H1 binds to the DNA as it enters and/or exits near the dyad axis of the nucleosome [14,15]. Early studies suggest that H1 can also bind to the non-canonical nucleosome free DNA ie., naked DNA and promoter regions during its exchange on chromatin [16,17]. Clark and Thomas studied the cooperative binding of H1 (heterogeneous) to the linear DNA indirectly by detecting the aggregate formation which is monitored by centrifugation and/or electron microscopy [18]. More recently, Mamoon *et al.*, investigated the primary binding of H1^0, its C- and G- domain to DNA using direct approaches like thermal denaturation studies and sedimentation velocity assays. Their equilibrium binding data strongly supports an allosteric transition of DNA from a lower affinity to a higher affinity form upon H1 binding rather than

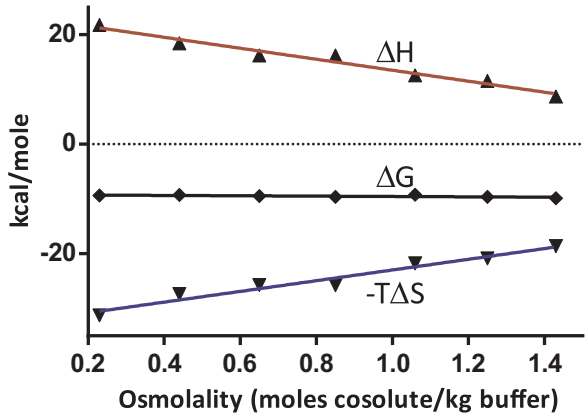

Fig. 6. A plot of the thermodynamic parameters, ΔG, ΔH, and -TΔS for the binding of $H1^0$ to CT-DNA as a function of osmolyte concentration.

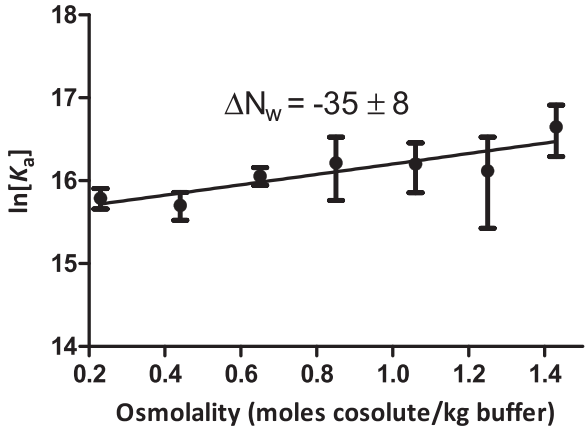

Fig. 7. A plot of ln[K_a] vs osmolyte concentration (moles of TEG/kg buffer) for the binding of $H1^0$ to CT-DNA. The data for $H1^0$ are shown as -•-.

cooperative binding [5,19]. In our studies, we tried to thermodynamically characterize the interactions of H1 to polymerized calf-thymus DNA using isothermal titration calorimetry. Although using nucleosomes may have provided a better binding substrate for H1, using linear DNA seems to provide a consistent picture with respect to the intrinsic binding affinity (K_a), as well as the enthalpy (ΔH) and entropy (ΔS) changes, and binding site size. A recent examination of H1 interactions with a 197 bp nucleosome revealed that when in complex with the nucleosome core, the globular domain of $H1^0$ is within contact

Table 3
Thermodynamic parameters for binding the complete $H1^0$ protein and its carboxyl terminal domain ($H1^0$-C) to CT-DNA.

	ΔG° (kcal/mol)	ΔH° (kcal/mol)	-TΔS° (kcal/mol)	Binding site Size (bp)	Molecular weight (kDa)
$H1^0$	−9.35	21.8 ± 0.2	−31.1	36	20.8
$H1^0$-C	−9.38	20.6 ± 0.2	−30.0	28	9.6
$H1^0$-G	−10.9*	1.1*	−12.0*	7	9.3

ITC derived thermodynamic parameters for binding the complete $H1^0$ protein and its carboxyl terminal domain ($H1^0$-C) to CT-DNA as determined previously [4]. Effective binding site size in base pairs was calculated from the titration endpoint, the DNA concentration in base pairs and the assumption that saturation stoichiometry is 1:1 (H1/DNA site).

distance of seven nucleotides within the core. [20] They report that the core DNA is the primary binding surface of the globular domain and the stoichiometry is consistent with the 7 bp binding site size that we determined for $H1^0$-G binding to CT-DNA. They also asserted that the $H1^0$ footprint on DNA to be 27–44 bp, [20] which is consistent with binding either the C domain (we determined $H1^0$-C binding site size of 28 bp) [4] or the full length protein (we determined $H1^0$ binding site size of 36 bp) [4]. We estimate from our naked DNA titration results that in the context of the nucleosome, binding of the $H1^0$- globular domain to the nucleosome core would occupy 7 DNA bp. This would place the globular domain in close contact with an additional three bp on each strand of linker DNA that is exiting the nucleosome and yield a total footprint for the nucleosome core $H1^0$-G interaction of 13 bp. Adding the $H1^0$-C interaction with one of the linker DNA tails (28 bp) yields a total $H1^0$ footprint of 41 bp. This result is in excellent agreement with the upper limit of the stoichiometry (44 bp) reported by Bednar *et al.* [20]

We previously reported that $H1^0$ and $H1^0$-C bind tightly to CT-DNA ($K_a \approx 1 \times 10^7$) (Table 3) [4]. In both cases the enthalpy change is highly endothermic (ΔH ≈ + 22 kcal/mol). Obviously the tight binding between $H1^0$ (including the C-terminus of $H1^0$, $H1^0$-C) and CT-DNA is driven by a large positive entropy change. The dependence of the complex formation constant, K_a, on ionic strength revealed that the electrostatic contribution to the free energy, ΔG_{elec}, accounts for only about 6–17% of the total ΔG. We also reported that the number of counterions released upon formation of the $H1^0$•CT-DNA complex is very small (< 1). In the current study, we have used ITC to further investigate the role of these dehydration effects on the binding of $H1^0$ to CT-DNA.

Based on the linear relationship between the ΔC_p and the changes in the solvent exposure of the hydrophobic and hydrophilic groups [21,22], we repeated the ITC binding experiments for $H1^0$ (or H^0-C)

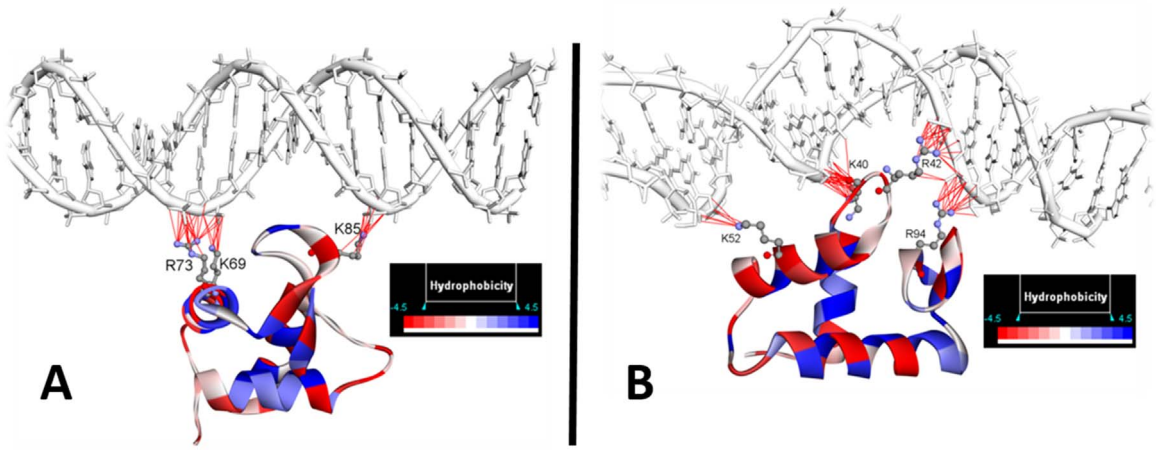

Fig. 8. A model for the proposed binding sites of $H1^0$-G interaction with ds-DNA. The protein is displayed using ribbon representation and colored according to the hydrophobicity of the residues. Intermolecular contacts are displayed as red wires.

Protein product 1: 86 amino acids
Molecular weight = 9349.1 Da

```
         10          20          30          40          50
ATDHPKYSDM IVAAIQAEKN RAGSSRQSIQ KYIKSHYKVG ENADSQIKLS
         60          70          80
IKRLVTTGVL KQTKGVGASG SFRLAKGDEP KRSVAF
                                    |____truncated in protein product 2
```

Protein product 2: 81 amino acids
Molecular weight = 8787.8 Da

```
         10          20          30          40          50
ATDHPKYSDM IVAAIQAEKN RAGSSRQSIQ KYIKSHYKVG ENADSQIKLS
         60          70          80
IKRLVTTGVL KQTKGVGASG SFRLAKGDEP K
```

Scheme 1. Sequence analysis for two protein products observed in HPLC trace from Fig. 5.

with CT-DNA at multiple temperatures and under varying solvent conditions. Both $H1^0$ and $H1^0$-C exhibit a strong and similar temperature dependence of ΔH and a negative heat capacity change (ΔCp = −430 cal mol^{-1} K^{-1}). Negative heat capacity changes are often attributed to the release of water molecules from the interface between the protein and DNA. However, there has been an argument that the water release alone is not sufficient to account for the change in heat capacity [23]. Eftink et al. studied the interaction between cytidine 3′-phosphate (3′-CMP) with RNAse A and also observed a negative heat capacity change for the formation of the complex. They attributed their ΔCp observation to the possibility of a ligand-induced change in the conformation of the protein [24]. Our observed negative heat capacity change values for the binding of $H1^0$ to CT-DNA are in agreement with other literature values for non-sequence-specific DNA binding proteins. [25,26] It is well known that sequence specific protein-DNA interactions involving tight and solvent excluded interfaces are often associated with very large negative heat capacity changes (about several thousand cal mol^{-1} K^{-1}) for the binding event [27–29].

The formation of a single complex was previously observed for the binding of either $H1^0$ or $H1^0$-C to CT-DNA. However, in this work binding of $H1^0$-G to CT-DNA at higher temperatures (303, 308, and 313 K) clearly shows the formation of two different complexes with characteristic thermodynamic signatures.

ITC experiments carried out at higher temperatures demonstrate that $H1^0$-G binding to CT-DNA results in exothermic enthalpy changes for complex formation. A two-fractional-sites model was used to fit the $H1^0$-G CT-DNA titration data. The enthalpy changes for formation of the two $H1^0$-G•CT-DNA complexes exhibit very different values (ΔH_1 = −2.9 kcal/mol and ΔH_2 = −8.1 kcal/mol) at 313 K but converge to essentially the same value (ΔH_1 = 1.2 kcal/mol and ΔH_2 = 0.9 kcal/mol) at 298 K. The heat capacity change for the formation of the lower affinity complex at 313 K assumes a large negative value (ΔCp = −590 cal mol^{-1} K^{-1}). The enthalpy change for binding the complete protein $H1^0$ to CT-DNA appears to obey Hess's law; in effect, the sum of enthalpy changes for the binding of individual $H1^0$ domains ($H1^0$-C, $H1^0$-G and $H1^0$-N)) to CT-DNA equals the enthalpy change for binding the intact $H1^0$ protein to CT-DNA:

$$\Delta H_{H1^0 \cdot CT-DNA} = \Delta H_{H1^0-C \cdot CT-DNA} + \Delta H_{H1^0-G \cdot CT-DNA} + \Delta H_{H1^0-N \cdot CT-DNA}$$

The enthalpy change for the formation of the high affinity complex of $H1^0$-G, ΔH_1, is used to model the interaction of the restricted globular domain in the complete $H1^0$ protein and the ΔH for binding the N-terminal domain, $\Delta H_{H\hat{1}\text{-}N \cdot CT-DNA}$, is assumed to be approximately zero due to the N-terminal domain being very short. It is interesting that the untethered $H1^0$-G binds to CT-DNA with such high affinity, (extrapolated ΔG_{avg} value is −10.9 ± 0.9 kcal/mol at 298 K). The tethering of the globular domain between the N and C termini appears to restrict the globular domain interactions with CT-DNA resulting in a single binding event and consequently a reduced free energy of binding

It is important to point out that the globular domain of H5 protein and $H1^0$ protein are highly homologous with a sequence identity of 78%. More importantly, protein residues that are in contact with the DNA as proposed by Ramakrishnan are conserved from H5-G to $H1^0$-G. The LC/MS results shown in Fig. 5 clearly show that there are two protein products produced from the protein expression system. The second protein product has five residues (RSVAF) removed from the C-terminus (see Scheme 1).

Notably, none of these five truncated residues (RSVAF) are in close proximity of any of the contact residues proposed by Ramakrishnan. Therefore, the fractional binding observed in ITC experiments at 313 K is clearly not the direct consequence of the two protein products. Furthermore, results from ESI-MS and short oligonucleotide ITC experiments confirm the stoichiometry in these binding studies. This further supports our ITC fractional binding model. Our ITC result for binding of $H1^0$-G to CT-DNA is in agreement with Ramakrishnan's homology model which suggests that $H1^0$-G may have two DNA binding domains. Results from our modeling study suggest that $H1^0$-G is capable of binding to CT-DNA via two different orientations. In the first binding model (Fig. 8A), $H1^0$-G binds to CT-DNA in the major groove and does not require any DNA conformational change. In the second binding model (Fig. 8B), the DNA must be bent slightly in order to facilitate contacts with all proposed residues in the $H1^0$-G protein. This result seems to explain the more negative heat capacity change exhibited by the lower affinity $H1^0$-G•DNA complex (ΔCp = −590 cal mol^{-1} K^{-1}) as compared to the less negative heat capacity change that is associated with the formation of the higher affinity $H1^0$-G•DNA complex (ΔCp = −260 cal mol^{-1} K^{-1}). Our previous CD work seemed to suggest that any DNA structural changes accompanying the binding of $H1^0$-G are not observable. However, ligation assays done by Maria *et al.* revealed that binding of H1 globular domains causes some unwinding of superhelical DNA [30].

The dependence of equilibrium binding constant on water activity allowed us to estimate the net volume of released surface water upon complexation of $H1^0$ and CT-DNA. The free energies of $H1^0$ binding to CT-DNA are almost independent of TEG concentrations reflecting compensation of enthalpic and entropic terms. Osmotic stress studies yield an estimate of the hydration changes (ΔN_w) occurring upon formation of the $H1^0$•CT-DNA complex. The difference in hydration between the free $H1^0$ and free CT-DNA and the $H1^0$•CT-DNA complex is –35 ± 8; in effect, approximately 35 water molecules are released upon complex formation. The number of released water molecules is certainly within the range of other reported literature values for the number of water molecules released upon protein binding to their nucleic acid receptors. For example, *Escherichia* coli tryptophan repressor protein releases about 75 water molecules upon 1:1 dimer/DNA complexation [31]. Approximately 18 molecules of water are released upon TATA binding protein (TBP) binding to 14-bp oligonucleotide duplexes [32]. Another interesting osmotic stress experiment involves the

restriction endonuclease *Eco*RI. About 70 water molecules are released when *Eco*RI binds nonspecifically to duplex DNA; however, this number increases to 150 and even 200 water molecules released for *Eco*RI binding to a specific DNA sequence such as GAATTC or TAATTC [33]. Jezewska et al. recently reported the interactions between African Swine Fever Virus (ASFV) polymerase X and ssDNA. The primary binding event is characterized by a binding-site-size of 7 nucleotides per ASFC pol X, a small endothermic enthalpy change (ΔH = 3.1 ± 0.6 kcal/mol), a large favorable change in the entropy (ΔS = 33 ± 3.5 cal mol^{-1} K^{-1}), and a release of approximately 19 water molecules upon complexation [34]. Although there is no direct evidence for a DNA conformational change in our study, a conformational change in DNA cannot be the main contributor to the observed negative heat capacity change because the immobilization of bases leads to negative rather than positive entropy change [34].

In summary, binding of $H1^0$ and $H1^0$-C to CT-DNA is mostly driven by a favorable change in entropy and an unfavorable change in enthalpy. The negative heat capacity changes observed for the formation of the $H1^0$•CT-DNA, $H1^0$-C•CT-DNA, and $H1^0$-G•CT-DNA complexes must result from the desolvation of the protein•DNA binding interface and the water release is the principle contributor to the favorable entropy changes for complex formation.

Acknowledgements

EAL acknowledges financial support for the thermodynamic studies from the National Science Foundation (CHE 1518006). CGM acknowledges support of the DoEd GAANN program (P200A 120066).

Appendix A. Transparency document

Supplementary data associated with this article can be found in the online version at http://dx.doi.org/10.1016/j.bbrep.2017.09.009.

References

[1] N. Happel, D. Doenecke, Histone H1 and its isoforms: contribution to chromatin structure and function, Gene 431 (2009) 1–12.
[2] M. Orrego, I. Ponte, A. Roque, N. Buschati, X. Mora, P. Suau, Differential affinity of mammalian histone H1 somatic subtypes for DNA and chromatin, BMC Biol. 5 (2007) 22.
[3] J.A. Subirana, Analysis of the charge distribution in the C-terminal region of histone H1 as related to its interaction with DNA, Biopolymers 29 (1990) 1351–1357.
[4] V.R. Machha, J.R. Waddle, A.L. Turner, S. Wellman, V.H. Le, E.A. Lewis, Calorimetric studies of the interactions of linker histone H1(0) and its carboxyl (H1(0)-C) and globular (H1(0)-G) domains with calf-thymus DNA, Biophys Chem. 184 (2013), pp. 22–28.
[5] Naila M. Mamoon, Yuguang Song, S.E. Wellman, Binding of histone H1 to DNA is described by an allosteric model, Biopolymers 77 (2004) 9–17.
[6] F. Watanabe, Cooperative interaction of histone H1 with, DNA 14 (1986) 3573–3585.
[7] N.M. Mamoon, Y. Song, S.E. Wellman, Histone H10 and Its Carboxyl-Terminal Domain Bind in the Major Groove of DNA, Biochemistry 41 (2002) 9222–9228.
[8] S.E. Wellman, Y. Song, D. Su, N.M. Mamoon, Purification of mouse H1 histones expressed in Escherichia coli, Biotechnol. Appl. Biochem. 26 (Pt 2) (1997) 117–123.
[9] R.D. Wells, J.E. Larson, R.C. Grant, B.E. Shortle, C.R. Cantor, Physicochemical studies on polydeoxyribonucleotides containing defined repeating nucleotide sequences, J. Mol. Biol. 54 (1970) 465–497.
[10] V.H. Le, R. Buscaglia, J.B. Chaires, E.A. Lewis, Modeling complex equilibria in isothermal titration calorimetry experiments: thermodynamic parameters estimation for a three-binding-site model, Anal. Biochem. 434 (2013) 233–241.
[11] V. Ramakrishnan, J.T. Finch, V. Graziano, P.L. Lee, R.M. Sweet, Crystal structure of globular domain of histone H5 and its implications for nucleosome binding, Nature 362 (1993) 219–223.
[12] C.A. Angell, J.C. Tucker, Anomalous heat capacities of supercooled water and heavy water, Science 181 (1973) 342–344.
[13] V.A. Parsegian, R.P. Rand, D.C. Rau, Macromolecules and water: probing with osmotic stress, Methods Enzymol. 259 (1995) 43–94.
[14] Y.B. Zhou, S.E. Gerchman, V. Ramakrishnan, A. Travers, S. Muyldermans, Position and orientation of the globular domain of linker histone H5 on the nucleosome, Nature 395 (1998) 402–405.
[15] D. Pruss, A.P. Wolffe, Histone-DNA contacts in a nucleosome core containing a Xenopus 5S rRNA gene, Biochemistry 32 (1993) 6810–6814.
[16] J.J. Hayes, A.P. Wolffe, Preferential and asymmetric interaction of linker histones with 5S DNA in the nucleosome, Proc. Natl. Acad. Sci. USA 90 (1993) 6415–6419.
[17] T.J. Caron F, Exchange of histone H1 between segments of chromatin, J. Mol. Biol. 146 (1981) 513–537.
[18] D.J.Ca.J. THOMAS, Differences in the binding of Hl variants to DNA, Eur. J. Biochem. 178 (1988).
[19] D.B.S. Susan, E. Wellman, Jonathan B. Chaires, Preferential binding of Hle histone to GC-rich, DNA, biochemestry 33 (1994) 384–388.
[20] J. Bednar, I. Garcia-Saez, R. Boopathi, A.R. Cutter, G. Papai, A. Reymer, S.H. Syed, I.N. Lone, O. Tonchev, C. Crucifix, H. Menoni, C. Papin, D.A. Skoufias, H. Kurumizaka, R. Lavery, A. Hamiche, J.J. Hayes, P. Schultz, D. Angelov, C. Petosa, S. Dimitrov, Structure and Dynamics of a 197 bp Nucleosome in Complex with Linker Histone H1, Mol. Cell 66 (2017) 384–397 (e388).
[21] J.B. Chaires, Energetics of drug-DNA interactions, Biopolymers 44 (1997) 201–215.
[22] N.V. Prabhu, K.A. Sharp, Heat capacity in proteins, Annu. Rev. Phys. Chem. 56 (2005) 521–548.
[23] J.W. Schwabe, The role of water in protein-DNA interactions, Curr. Opin. Struct. Biol. 7 (1997) 126–134.
[24] M.R. Eftink, A.C. Anusiem, R.L. Biltonen, Enthalpy-entropy compensation and heat capacity changes for protein-ligand interactions: general thermodynamic models and data for the binding of nucleotides to ribonuclease A, Biochemistry 22 (1983) 3884–3896.
[25] J.E. Ladbury, J.G. Wright, J.M. Sturtevant, P.B. Sigler, A thermodynamic study of the trp repressor-operator interaction, J. Mol. Biol. 238 (1994) 669–681.
[26] Y. Takeda, A. Sarai, V.M. Rivera, Analysis of the sequence-specific interactions between Cro repressor and operator DNA by systematic base substitution experiments, Proc. Natl. Acad. Sci. USA. 86 (1989) 439–443.
[27] C. Bailly, G. Chessari, C. Carrasco, A. Joubert, J. Mann, W.D. Wilson, S. Neidle, Sequence-specific minor groove binding by bis-benzimidazoles: water molecules in ligand recognition, Nucleic. Acids. Res. 31 (2003) 1514–1524.
[28] B. Jayaram, T. Jain, The role of water in protein-DNA recognition, Annu. Rev. Biophys. Biomol. Struct. 33 (2004) 343–361.
[29] B. Madan, K.A. Sharp, Hydration heat capacity of nucleic acid constituents determined from the random network model, Biophys. J. 81 (2001) 1881–1887.
[30] M. Ivanchenko, A. Hassan, K. van Holde, J. Zlatanova, H1 binding unwinds DNA. Evidence from topological assays, J. Biol. Chem. 271 (1996) 32580–32585.
[31] M.P. Brown, A.O. Grillo, M. Boyer, C.A. Royer, Probing the role of water in the tryptophan repressor-operator complex, Protein Sci. 8 (1999) 1276–1285.
[32] S. Khrapunov, M. Brenowitz, Comparison of the effect of water release on the interaction of the Saccharomyces cerevisiae TATA binding protein (TBP) with "TATA Box" sequences composed of adenosine or inosine, Biophys. J. 86 (2004) 371–383.
[33] C.R. Robinson, S.G. Sligar, Changes in solvation during DNA binding and cleavage are critical to altered specificity of the *Eco*RI endonuclease, Proc. Natl. Acad. Sci. USA 95 (1998) 2186–2191.
[34] M.J. Jezewska, M.R. Szymanski, W. Bujalowski, Interactions of the DNA polymerase X from African Swine Fever Virus with the ssDNA. Properties of the total DNA-binding site and the strong DNA-binding subsite, Biophys. Chem. 158 (2011) 26–37.